Deliverable 3.4

Report on Quality Control and User Feedback

Project acronym: *AFFECTS*
Project Title: *Advanced Forecast For Ensuring Communications Through Space*
Grant Agreement number: *263506*
Coordinator: *Volker Bothmer*

Project co-funded by the European Commission, Seventh Framework Programme

Funding Scheme: *FP7-SPACE-2010-1*

Due date of deliverable:	February 28, 2013
Actual submission date:	March 29, 2013
Start date of the project:	March 1, 2011
Project duration:	3 years
Work package:	3 “Early Warning System”
Deliverable:	3.4
Lead beneficiary for this deliverable:	ROB
Editor:	A. Devos
Authors:	A. Devos, R. Viereck (NOAA-SWPC), C. Verbeeck, E. Robbrecht
Quality reviewer:	V. Bothmer (UGOE)

Project co-funded by the European Commission within the Seventh Framework Programme (2007)		
Dissemination level		
PU	**Public**	**PU**
PP	**Restricted to other programme participants (including the Commission Services)**	
RE	**Restricted to a group specified by the consortium (including the Commission Services)**	
CO	**Confidential, only for members of the consortium (including the Commission Services)**	

Document Control

This document has no controlled or maintained paper copies. The master document will be accessible through the AFFECTS website upon approval. Changes to this document will be made available to the scientific community through updates of this document at the AFFECTS website.

Issue record

Version	Date	Author(s)	Reason for modification	Status
1.0	29-03-2013	A. Devos, R. Viereck, C. Verbeeck, E. Robbrecht	NA	Submitted to AFFECTS PI
1.1	29-03-2013	V. Bothmer	Final review	

This report has been prepared under the scope of the AFFECTS project in collaboration of the following participants of Work Package 3 "Early Warning System" with Lead of ROB (Cis Verbeeck):

Georg-August-Universität Göttingen, Stiftung Öffentlichen Rechts, Germany (UGOE)
Phone: +49 551 39 5044, Fax: -5043, http://www.astro.physik.uni-goettingen.de/
Volker Bothmer, e-mail: bothmer@astro.physik.uni-goettingen.de

Royal Observatory of Belgium, Brussels, Belgium (ROB)
Phone: +32 2 890 98 19, Fax: +32 2 374 98 22, http://www.observatory.be/
Andy Devos, e-mail: andy.devos@oma.be
Cis Verbeeck, e-mail: cis.verbeeck@oma.be
Eva Robbrecht, e-mail: eva.robbrecht@oma.be

Tromsø Geophysical Observatory, University of Tromsø, Tromsø, Norway (UoT)
Phone: +47 77620884, http://uit.no
Chris Hall, e-mail: chris.hall@uit.no

Space Research Institute of the National Academy of Sciences and the National Space Agency, Ukraine (SRI NASU-NSAU)
Phone: +380 93 3264229, http://www.ikd.kiev.ua
Aleksei Parnowski, e-mail: parnowski@gmail.com

Fraunhofer-Gesellschaft zur Förderung der angewandten Forschung e.V., Germany (FHG)
Phone: +49 761 8857 310, http://www.ipm.fraunhofer.de
Raimund Brunner, e-mail: raimund.brunner@ipm.fraunhofer.de

German Aerospace Center, Institute of Communications and Navigation, Neustrelitz, Germany (DLR)
Phone: +49 3981 480 215, http://www.dlr.de/kn/en/desktopdefault.aspx/tabid-2053/
Jens Berdermann, e-mail: jens.berdermann@dlr.de

Space Weather Prediction Center of NOAA, USA (NOAA-SWPC)
Phone: +1 303 497 7348, Fax: +1 303 497 3645, http://www.swpc.noaa.gov/
Rodney Viereck, e-mail: rodney.viereck@noaa.gov

Content

1. Introduction

This present document consists of three parts. The first part concerns the forecast verification performed at the Royal Observatory of Belgium. Secondly, an overview is provided of several space weather products developed and validated at the Space Weather Prediction Center of the National Oceanic and Atmospheric Administration. Finally we report on the user feedback provided by the attendees of the AFFECTS User Workshop.

2. Forecast Verification at ROB

2.1 Introduction

Since the year 2000 the Royal Observatory of Belgium (ROB) has the responsibility of Regional Warning Center (RWC). About 8 space weather forecasters are responsible for the forecasting on a weekly schedule. Every day a forecast is sent with a prediction of a few space weather parameters for the next days.

This section describes the comprehensive verification analysis of the space weather forecasts carried out by the RWC in Belgium. The space weather forecast verification analysis involves not only the quality control or performance analysis of the forecasting, but also more broadly the analysis of verification measures. According to [Jolliffe and Stephenson] a verification measure is any function of the forecasts, observations or their relationship. An example could be the probability of an event being observed, which is determined independently of the correspondence between forecasts and observations.

The verification analysis involves descriptive statistics about forecasts and observations, regardless of their relationship. The conditional statistics, error analysis and performance measures assess the strength of the correspondence between observations and forecasts. This information mostly is visualized in specific figures.

Section 2 covers the analysis of the forecast of the 10.7 cm solar flux, while section 3 describes the evaluation of the geomagnetic forecast. In both cases the forecast performance is compared to that of common numeric models. The last section summarizes the obtained results and mentions a few next steps.

2.2 Forecast verification of F10.7

2.2.1 What is F10.7?

The F10.7 or 10.7 cm solar flux is widely used as an indicative parameter for solar activity. It measures the solar radio emission at a wavelength of 10.7 cm and is closely related to the International Sunspot Number (ISN) [SIDC, Tapping and Charrois]. The F10.7 is measured daily by the National Research Council of Canada in Pentincton. The solar flux has a minimum of 64 sfu and an undefined maximum (1 solar flux unit or sfu is 10^{-22} W m^{-2} Hz^{-1}).

2.2.2 Setup of the verification analysis

At the RWC in Belgium, the F10.7 is forecasted daily for the current day and the next two days. The forecaster on duty estimates these values based on the values of the days before, taking into account different influences. Due to the solar rotation, active regions (ARs) near the west limb will have no contribution to the solar flux within a few days, while the emissions of ARs behind the east limb will be added in the next days. As the Sun rotates, flux emitted in the direction of the Earth is added or subtracted by active regions becoming visible or invisible.

This task remains difficult, since active regions might become more (or less) active and as such emit more (or less) flux at the specific radio wavelength. Moreover, the observed solar flux might be influenced by a (strong) solar flare at the time of measurement.

Despite the complicating factor, a few simple numerical models are defined to provide an estimate of the solar flux:

- The **persistence model** assumes solar activity will stay at the same level as yesterday. The solar flux of today is estimated to be exactly the same as the value of yesterday.

- The **recurrence model** focusses on the influence of the Carrington rotation (CR) of on average 27 days. The recurrence model assumes the active regions are as active as a full rotation ago and estimates the solar flux as the flux value of 27 days ago. In addition also a recurrence model with a time shift of 14 days, which is half a rotation, was tested. The argument is that active regions at the west limb reoccur at the east limb about 14 days later.

- The **corrected recurrence model** seeks a compromise between the persistence and recurrence model. This model looks at the daily increment of 27 days ago and applies this to the solar flux of yesterday. The corrected recurrence model focusses on the latest measurement (of yesterday) and combines this with the estimated flux change as it occurred one rotation ago. Similarly as for the recurrence model, the corrected recurrence model was applied with a time shift of 14 days and 27 days.

- As last numeric technique **a linear model** is implemented, which estimates the linear trend of the past days and applies that to the flux for today and the next two days. A linear regression model with a constant is used, using the observations of the past 4 days.

The verification analysis could provide insight in the strengths and weaknesses of the manual forecast versus the numerical models. The results should inform us which model is most appropriate in several situations, like a high versus low flux value or at solar maximum or solar minimum for days 1, 2 and 3.

2.2.3 Analysis of the observations and forecasts

At the RWC in Belgium the solar flux is forecasted since 2002. Figure 1 visualizes the evolution of the monthly average forecasted solar flux by SIDC on day 1, 2 and 3 as well as the observations. Clearly the influence of the solar cycle is visible, with a higher average flux close to solar maximum and very low values near the minimum in December 2008. As expected, the monthly average forecast for day 1 more closely follows the observations than those for days 2 and 3.

Table 1 provides an overview of a few basic statistical measures of the observations and different forecasts. Note that the number of data is not exactly the same for each of the forecasts. For example, the persistence model needs the observation of the past day, making it inapplicable for the first day of a period. Similarly, the linear regression model requires the past 4 values, which are only available from day 5. The recurrence model with a delay of 27 days (similar for 14 days) can only be applied from 27 (or 14) days on after the first observation in the considered period. In addition, the SIDC forecast has a few cases less than the observation due to unavailability of the forecast.

The mean values of the SIDC forecast are slightly higher than the mean of the observations and even of all other forecasts. This indicates the SIDC forecast in general is overestimating the flux. The mean SIDC forecast is larger at days 2 and 3 than on day 1, in contrast to most numerical models. The univariate statistics included in Table 1 of the persistence and (uncorrected) recurrence models are independent of the day, since (roughly) the same sample, up to a specific time shift, is used for days 1, 2 and 3.

The skewness is higher on days 2 and 3 than day 1 for the corrected recurrence and the linear fit models, corresponding to heavier tails at the high flux values. This could be related to the fact that these models are based on the differences or trend in the observations of the previous days. At large flux values the day-to-day differences may be very large and in case of a monotonic increasing trend, the model could provide very high forecasted flux values. This especially holds for the linear fit, a method which is known to be sensitive to individual observations, an effect enhanced by the low number of time points regression is based on [Chatterjee and Hadi].

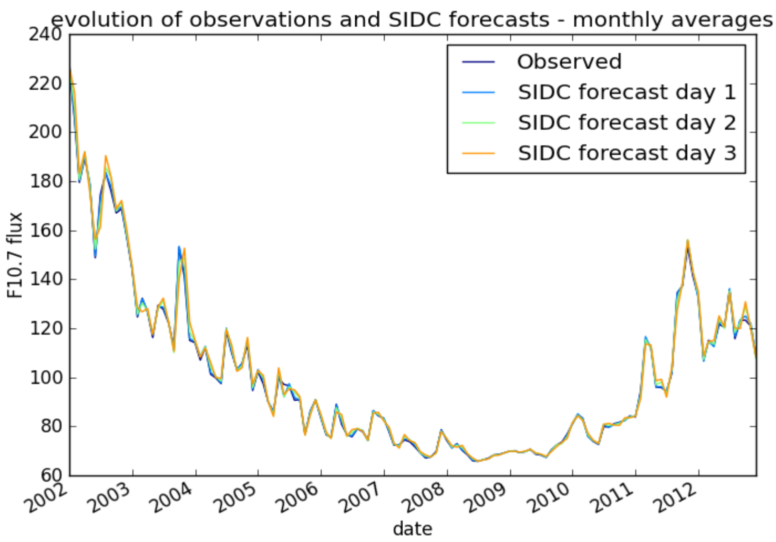

Fig. 1: The evolution of the monthly averages of both the observations and SIDC forecasts from 2002 till 2012.

The higher skewness for the linear regression slightly is reflected in Figure 2 showing higher probabilities at flux values above 200 sfu compared to other forecasts. Both the SIDC forecast and persistence model show a stronger linear relationship with the observations than other models. This is in correspondence to the correlations with the observations (see Table 1). The lowest correlations are obtained by the uncorrected recurrence models, which justifies not to include these models in most of the remaining output. For all other models the correlation is worse for days 2 and 3 than for day 1.

	Observed	SIDC forecast			Persistence			Recurrence 14 days			Recurrence 27 days			Corrected recurrence 14 days			Corrected recurrence 27 days			Linear fit		
		day 1	day 2	day 3	day 1	day 2	day 3	day 1	day 2	day 3	day 1	day 2	day 3	day 1	day 2	day 3	day 1	day 2	day 3	day 1	day 2	day 3
count	4018	4016	4015	4014	4017	4016	4015	4004	4005	4006	3991	3992	3993	4003	4003	4003	3990	3990	3990	4014	4013	4012
mean	101.16	101.41	101.61	101.79	101.15	101.15	101.15	101.12	101.13	101.13	101.10	101.10	101.10	100.71	100.68	100.65	100.30	100.26	100.23	101.03	101.00	100.97
standard deviation	36.29	36.69	36.98	37.30	36.29	36.30	36.30	36.34	36.34	36.34	36.40	36.39	36.39	35.98	36.63	37.62	35.30	35.70	36.18	36.94	37.96	39.29
skewness	1.509	1.524	1.524	1.527	1.509	1.509	1.509	1.510	1.510	1.510	1.510	1.510	1.511	1.498	1.511	1.524	1.490	1.511	1.522	1.562	1.627	1.694
correlation with observation	1.000	0.991	0.966	0.929	0.990	0.975	0.955	0.766	0.767	0.772	0.869	0.869	0.866	0.976	0.957	0.935	0.982	0.969	0.952	0.988	0.970	0.944

Table 1: A few descriptive statistics for the observations and each of the forecasts, for days 1, 2 and 3.

	Ob-served	SIDC forecast			Persistence			Recurrence 14 days			Recurrence 27 days			Corrected recurrence 14 days			Corrected recurrence 27 days			Linear fit		
		day 1	day 2	day 3	day 1	day 2	day 3	day 1	day 2	day 3	day 1	day 2	day 3	day 1	day 2	day 3	day 1	day 2	day 3	day 1	day 2	day 3
count	4018	4016	4015	4014	4017	4016	4015	4004	4005	4006	3991	3992	3993	4003	4003	4003	3990	3990	3990	4014	4013	4012
mean abso-lute error	0.00	0.24	0.46	0.68	0.03	0.06	0.09	0.38	0.35	0.32	0.76	0.72	0.69	0.00	-0.03	-0.06	0.00	-0.03	-0.06	-0.01	-0.01	-0.02
rmse	0.00	4.96	9.53	13.87	5.17	8.15	10.90	24.64	24.62	24.38	18.35	18.36	18.55	7.83	10.61	13.30	6.68	8.82	11.10	5.70	9.21	13.06
skill score	1.00	0.08	-0.37	-0.62	0.00	0.00	0.00	-21.71	-8.13	-4.00	-11.59	-4.08	-1.90	-1.29	-0.69	-0.49	-0.67	-0.17	-0.04	-0.22	-0.28	-0.44
1% quan-tile of errors	0	-13	-27	-42	-15	-24	-33	-72	-70	-69	-53	-53	-56	-23	-31	-39	-19	-26	-32	-15	-24	-35
5% quan-tile of errors	0	-7	-15	-21	-8	-13	-17	-37	-39	-39	-29	-30	-29	-12	-16	-21	-10	-14	-17	-8	-14	-20
10% quan-tile of errors	0	-4	-10	-14	-5	-8	-12	-25	-25	-25	-17	-18	-18	-8	-11	-14	-7	-9	-12	-5	-9	-13
25% quan-tile of errors	0	-1	-3	-4	-2	-2	-3	-8	-8	-8	-5	-5	-5	-3	-4	-5	-2	-3	-4	-2	-3	-5

75% quan-tile of errors	0	2	4	6	2	3	4	9	9	9	8	8	8	3	3	4	2	3	4	2	3	4
90% quan-tile of errors	0	5	10	15	5	8	11	27	27	26	21	21	20	8	11	14	7	9	12	6	9	13
95% quan-tile of errors	0	8	16	22	8	12	16	40	40	39	30	30	30	12	17	21	11	14	18	9	14	21
99% quan-tile of errors	0	15	28	41	16	24	30	68	67	66	45	45	47	21	30	38	19	26	32	18	28	41

Table 2: A few statistics on the errors of each of the forecasts to the observations, for days 1, 2 and 3.

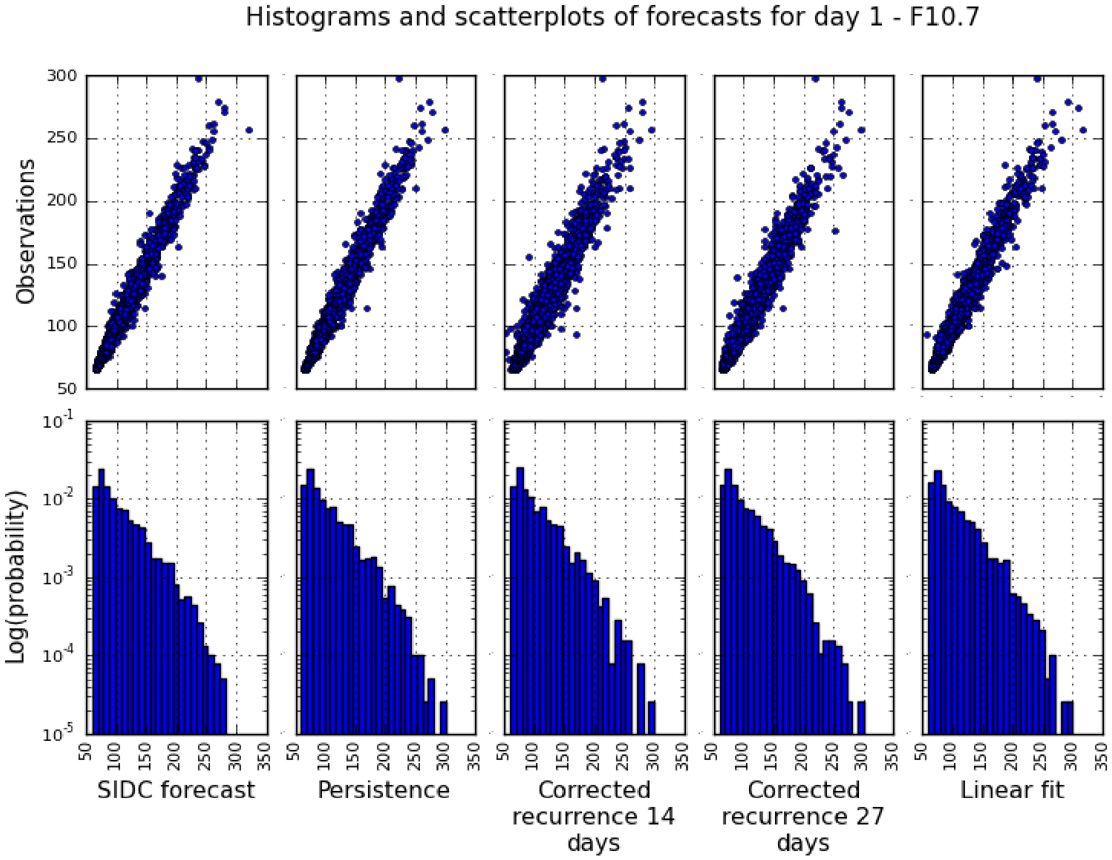

Fig. 2: Matrixplot combining (log scaled) histograms (bottom row) and scatterplots (top row) of several forecasts for day 1. The same plots for days 2 and 3 can be obtained from the SIDC website http://www.sidc.be/forecastverification.

2.2.4 Error analysis

To go a step further, an error analysis is performed. Table 2 mentions the mean error, rmse, skill score and several quantiles of the errors. The root mean squared error (rmse) is defined as: $\sqrt{\frac{1}{N-1}\sum_i (f_i - o_i)^2} = \sqrt{mse}$,

and the skill score is defined as: $1 - \frac{mse}{mse_{ref}}$, range $(-\infty, 1]$

in which $mse_{ref} = mse_{persistence}$ the mse of the reference model, the persistence model in this case. The closer the skill score is to +1, the better the model performs on average. A forecast with a skill score of 0 has the same mse as the reference model.

The mean absolute error is the error in a non-relative sense. The quantile is a value that separates an ordered sample in two parts, one part with lower values and the other part with higher values. For instance, the 10% quantile separates the lowest 10% of the sample from the 90% that is higher.

The skill score for the SIDC forecast is highest on day 1, indicating on average the best performance among the discussed models. The skill score is worse on day 2 and 3. Apart from the uncorrected recurrent models, the SIDC forecast provides the worst skill score for day 3. On day 1, the quantiles for the SIDC forecast are very similar to that of the persistence model, and better than those of the corrected recurrence and linear fit models. For days 2 and 3 the range of the errors, quantified by the quantiles, at best approach those of the corrected recurrence and linear fit models.

The evolution of the average monthly errors is displayed in Figure 3. The errors are much larger at the time of solar maximum than at solar minimum. That holds especially for days 2 and 3, but also for day 1 some large average errors occur, for example at mid 2005 and the end of 2011.

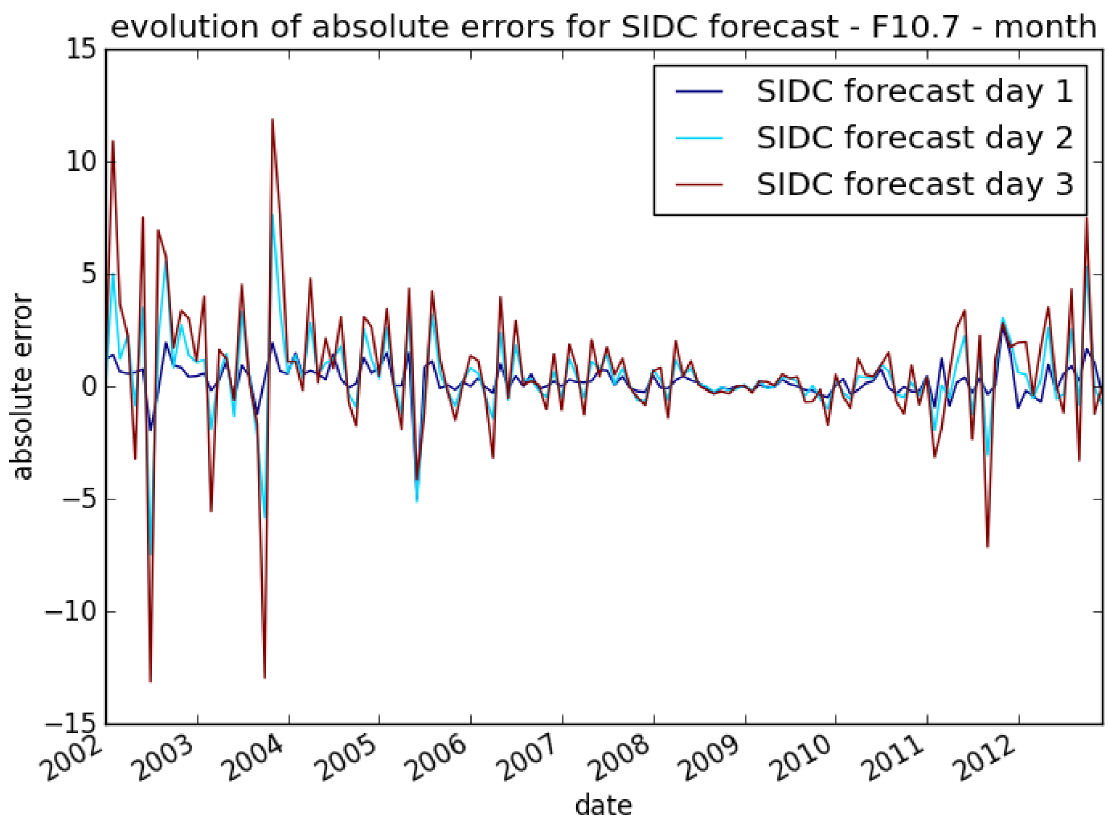

Fig. 3: Evolution of the average monthly errors of the SIDC forecast along the period 2002-2012 for days 1, 2 and 3.

It is of interest to determine the size of the errors conditional on the observed flux values. Therefore the conditional quantiles of the errors are studied. In Figure 4 the histogram of the observations is shown as well as the conditional median error and the conditional interquartile range (IQR) of the errors for the forecasts on day 1. The IQR is defined as the range between the 25% and 75% quantile : $IQR = Q_3 - Q_1$, in which Q_1,Q_3 respectively are the 25% and 75% quantile or also called the 1st and 3rd quartile.

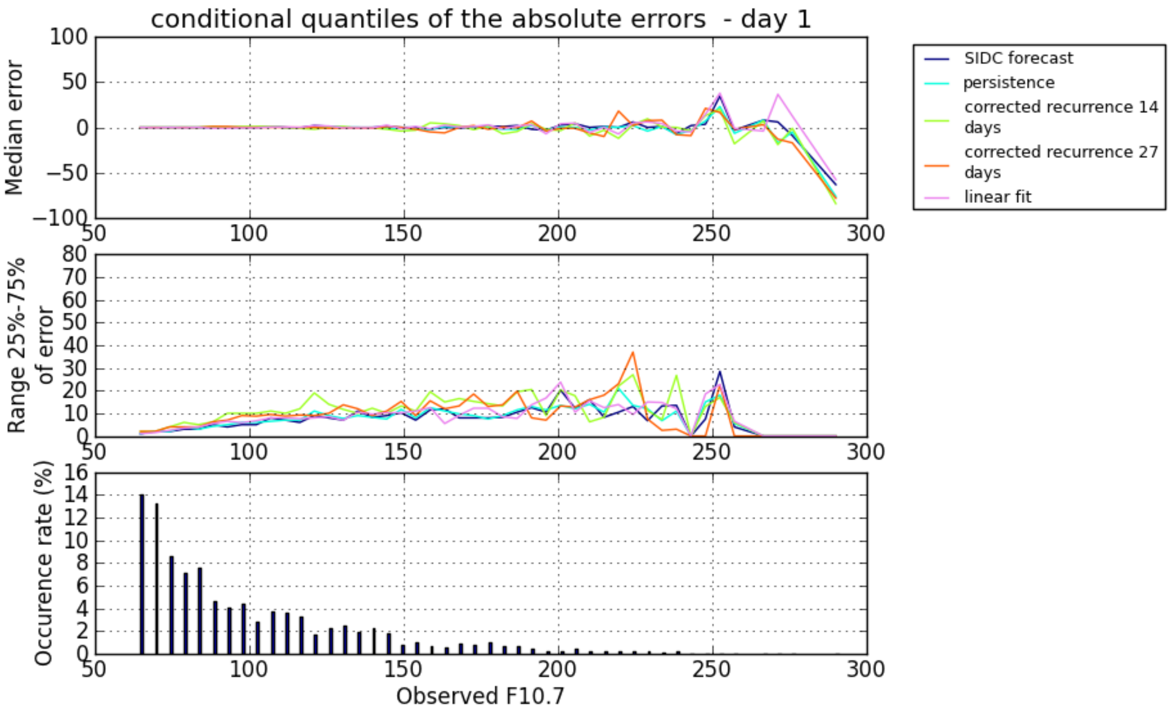

Fig. 4: Conditional errors for day 1: histogram of the observed F10.7 (bottom), combined with the conditional median error (top) and the conditional IQR of the errors (middle) for the SIDC forecast, persistence model, corrected recurrence models for 14 and 27 days and linear fit. The full period from 2002 onwards is covered.

The conditional median error can be interpreted as the typical error given a specific observed flux value. Given an observed flux of 200 sfu, the SIDC forecast has in half of the cases an error below (roughly) 0 sfu and in the other half of the cases above 0 sfu. At a flux of 200 sfu, the conditional IQR of the errors is about 20 sfu for the SIDC forecast, which implies half (between the 1st and 3rd quartile) of the errors are in a range of 20 sfu around the median error. Hence, in case of 200 sfu, half of the forecasts are at $200 \pm \frac{20}{2}$ sfu. At an observed flux of 250 sfu, the median error is roughly 30 sfu, though this is based on only very few cases.

Comparison of the different methods, reveals that the median error is pretty flat till a value of 150 sfu, meaning as many positive as negative errors occur for all models. Furthermore, the persistence model and the SIDC forecast both have a moderate median error around 0 sfu till a flux of almost 250 sfu. At extreme flux values around 250 sfu and more, errors get very large.

On days 2 and 3 (figures 5 and 6), errors on the flux clearly are higher, even at an observed flux of 150 to 200 sfu. At day 3, the IQR of the errors for the SIDC forecast easily gets double as broad as on day 1. At a flux of 200 sfu, the IQR of the errors is about 40 sfu. While for day 1 the corrected recurrence models reach higher errors (especially visible in the IQR), for day 3 the conditional errors are mainly lower than for the other models.

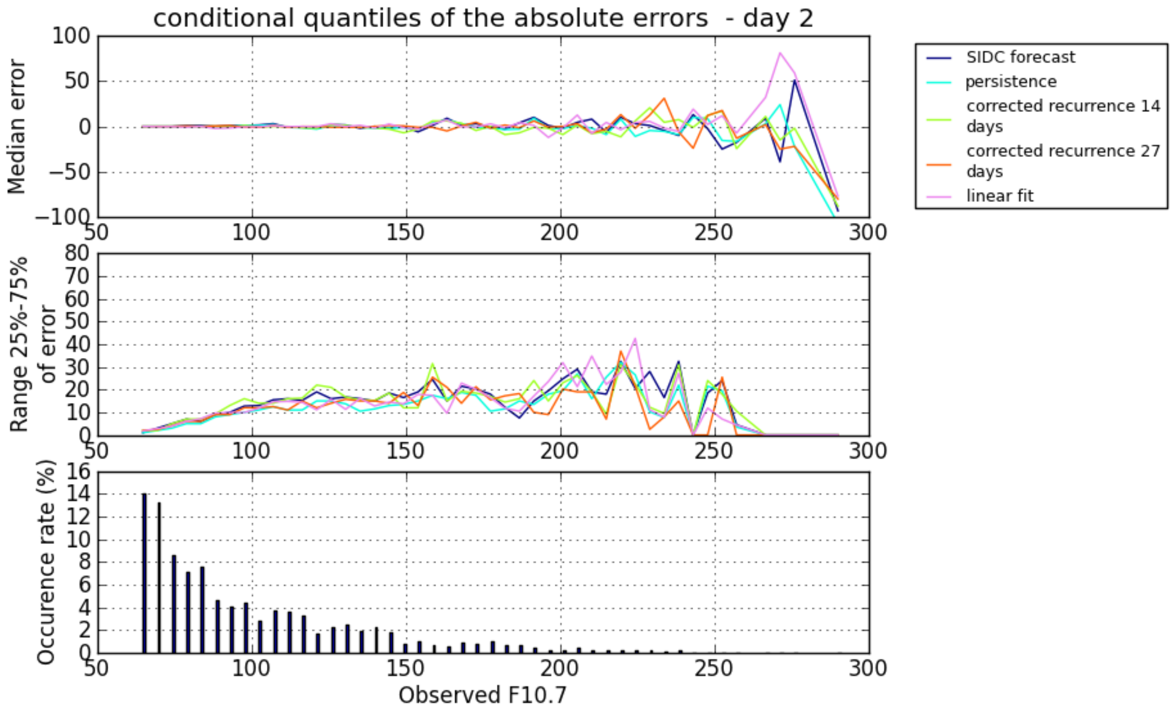

Fig. 5: Conditional errors for day 2.

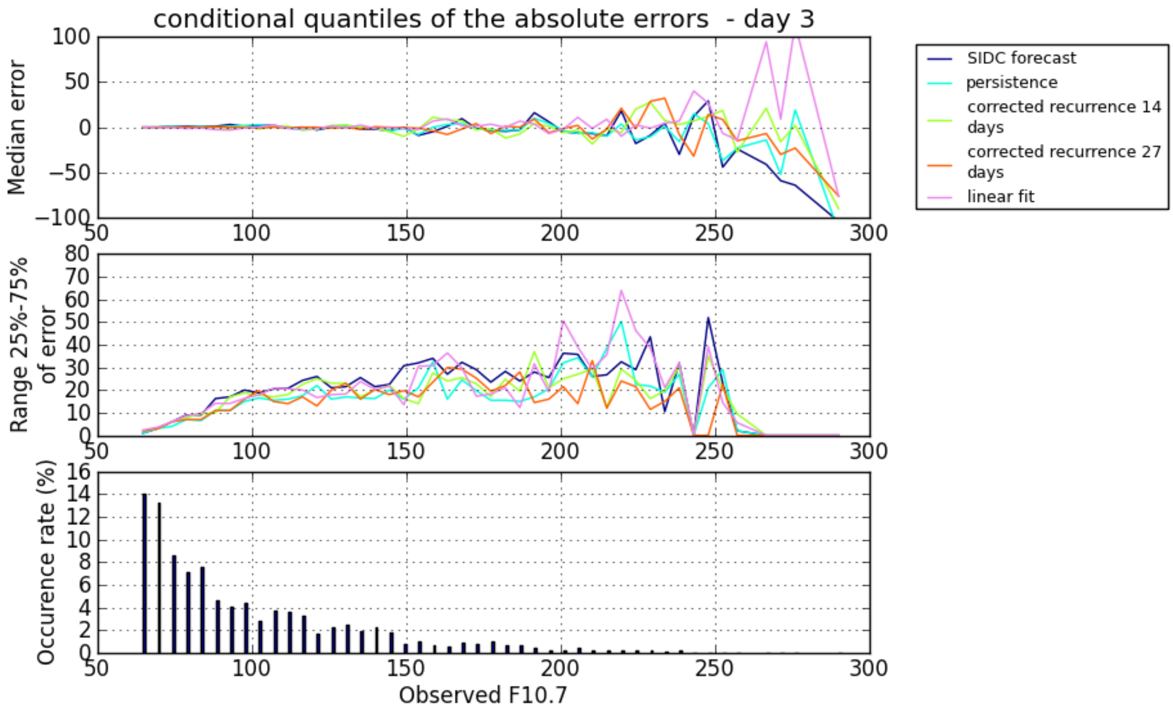

Fig. 6: Conditional errors for day 3.

The different models can also be compared by their average errors, independent of the observations. As already quantified in table 2, the skill score for the SIDC forecast on day 1 is higher than for the numerical models, but is worse for days 2 and 3 compared to most models. This is visualized in Figures 7 and 8. Both figures plot aggregate information on the errors as well; in Figure 7 the mean absolute errors, while in Figure 8 the mean absolute value of these errors are displayed. In other words, in Figure 8 the unsigned errors are averaged. Interpretation of both plots together reveals that though the SIDC forecast has a higher mean error, the mean unsigned error is about as good as for the corrected recurrence and linear fit models, certainly for days 1 and 2. The mean unsigned error is similar (day 1) or only slightly inferior (day 2) to the persistence model. This implies that the errors made by the SIDC forecast are not really worse than those of the numerical models (for days 1 and 2). In addition the errors concentrate more on the positive side with respect to the numerical models, revealing more overestimation than underestimation of the solar flux.

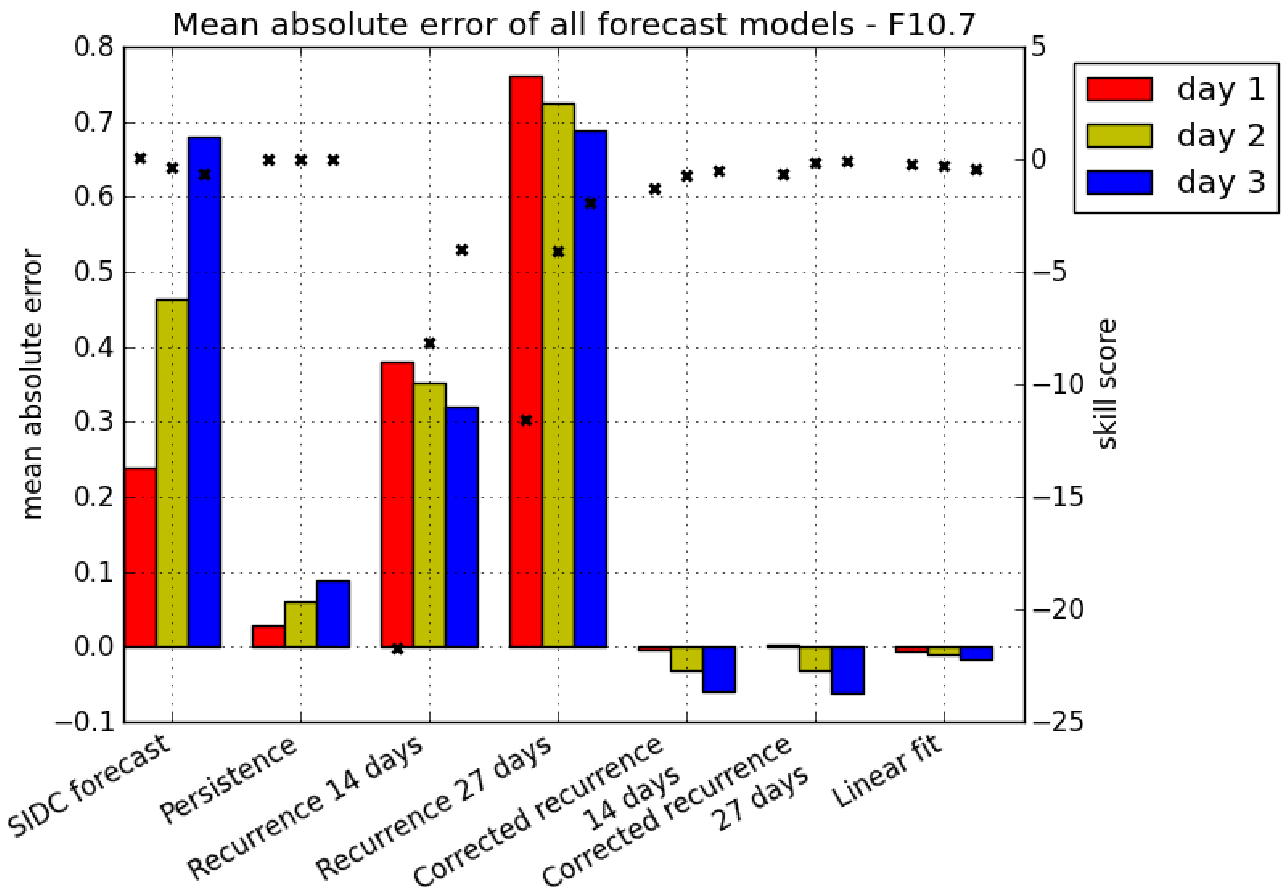

Fig. 7: Mean errors (bars) and skill scores (crosses) for the different methods (days 1, 2 and 3).

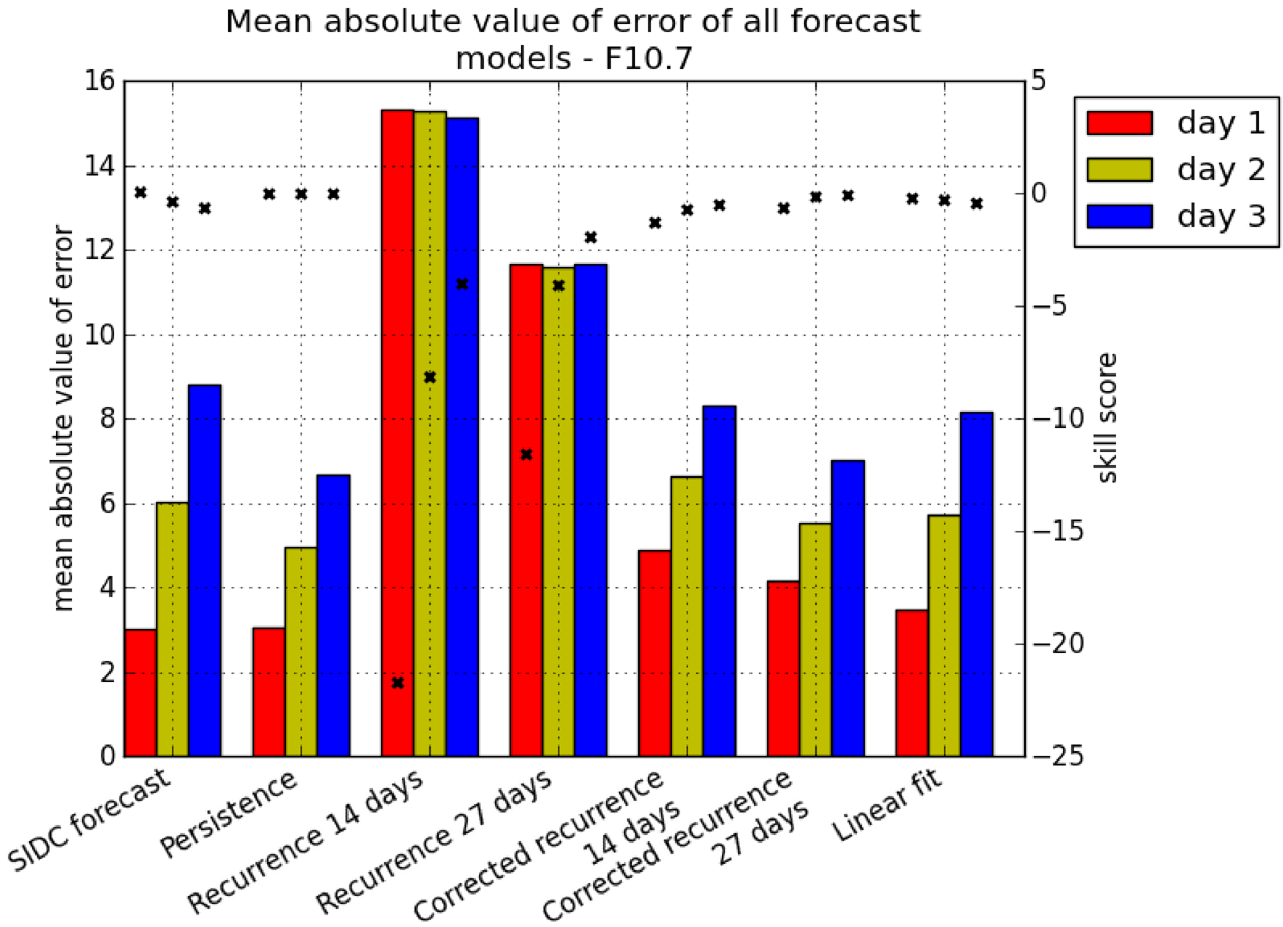

Fig. 8: Mean absolute value of the errors (bars) and skill scores (crosses) for the different methods (days 1, 2 and 3).

2.3 Forecast verification of the geomagnetic index

2.3.1 What is the K-index?

The solar wind and CMEs disturb the Earth's magnetic field. The degree of perturbation can be quantified by the geomagnetic index K. The K-index ranges from 0 to 9, with 0 being quiet and 9 extreme geomagnetic storm. At several regional centers around the world the local K-index is measured. The planetary K_p index is calculated as a weighted average of K-indices from a defined network of regional geomagnetic observatories. At the RWC in Belgium the local K-index from Dourbes (50.10°North, 4.58°East), Belgium is forecasted.

In practice the K-index is measured every 3 hours and since June 2004 a forecast is provided for these time slots. The verification analysis calculates the maximum K-value (from these 3-hourly values) for the next 48 hours from 12h30 UT onwards. Unless stated differently, the maximum K-index across the next 48 hours was analyzed.

Unfortunately, the local K-index from Dourbes has many data gaps. The local K-index from Chambon-la-Forêt (48.06°North, 2.30°East) is more reliable. In order to use as many data as possible, the K-index from Chambon-la-Forêt is used for the verification analysis. This can be justified by the small difference in their geographical coordinates.

2.3.2 Setup of the verification analysis

The K-index can be estimated by numerical models, similarly as for the solar flux. The human forecast at SIDC was compared to the following techniques (section 2.2 for detailed explanation):

- The recurrence model with a delay of both one Carrington rotation (27 days) and half a rotation (14 days).

- The corrected recurrence model with a delay of both one Carrington rotation (27 days) and half a rotation (14 days).

- The climatology model, predicting the geomagnetic index as the average across the past 30 days, assuming the K-index is not influenced by short term fluctuations (on a time scale of days, weeks).

Note that the persistence and linear model were not retained for the K-index. The persistence model is less appropriate for the K-index since CME effects could cause abrupt changes in the observations. The linear regression is not feasible to apply on a discrete set of values, with a tiny data range of 0 to 9.

The analysis can be organized in three small parts, which will be elaborated on further in the next sections:

- Evolution of the observational and forecasted K-index

- The geomagnetic index is treated as a 'continuous' value, for which the error analysis could be applied as for the solar flux

- The geomagnetic index could be dichotomized (or categorized) to analyze the data as a binary event (or forecast).

2.3.3 Analysis of observations and forecasts

The average monthly observed and forecasted K-index is displayed in Figure 9. The average K-index roughly follows the solar cycle with the lowest K-index in 2008-2009, near the solar minimum of solar cycle 23. Several peaks occur in this graph, both for the observations and forecasts. Unfortunately, these peaks often do not coincide, for example in 2004, first half of 2006, mid 2007 and begin 2011, indicating we have large errors in these periods.

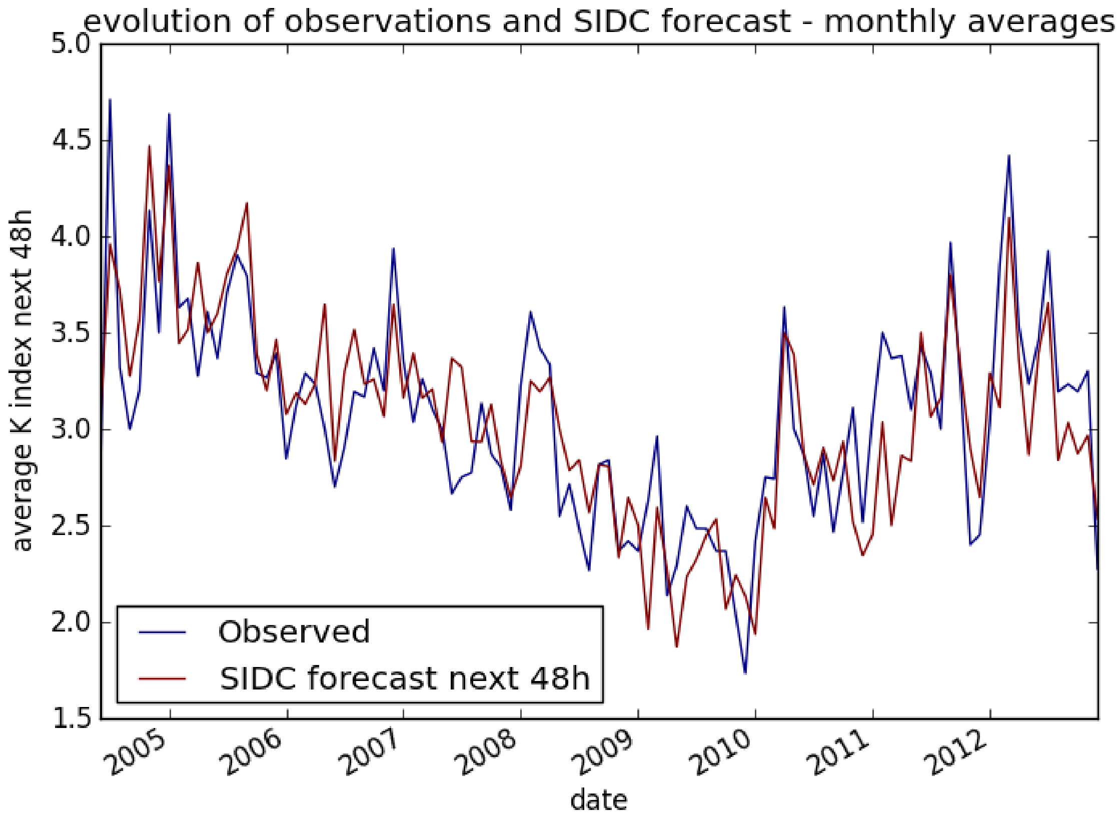

Fig. 9: Average monthly observational and SIDC forecasted K-index.

Figure 10 presents a matrixplot combining histograms and color grids of several forecasts. The histogram of the observations and the SIDC forecast resemble most, while the climatology model results in the most deviating distribution with a strong peak near K=3, which is occurring most frequently. This is quite logical given the definition of the model. The color grids on the top row indicate that the corrected recurrence models as well as the SIDC forecast provide a linear relationship with the observations. The plots on the second row indicate that many high K-values (8,9) are underestimated by the SIDC forecast, which occurs less for the corrected recurrence models. Similarly, in the rare cases a high K-index was forecasted, the observational value mostly is slightly lower, which happens for the corrected recurrence models as well as the SIDC forecast.

An observation of K=0 is always overestimated by the SIDC forecast (and the climatology model), since we hardly have forecasted K=0 in the period 2004-2012.

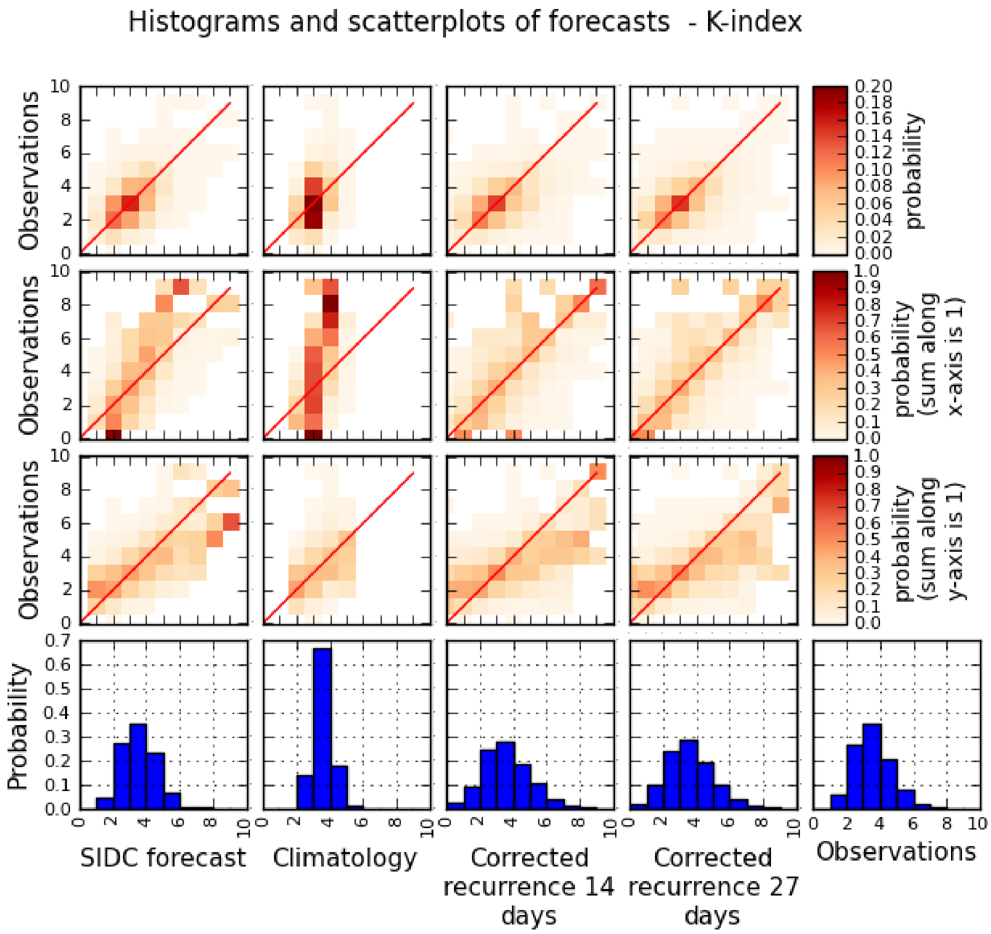

Fig. 10: Matrixplot combining histograms (bottom row) and color grids (3 top rows) of several forecasts (SIDC, climatology, corrected recurrence at 14 and 27 days). The top row contains the color grid, with a normalization of the probabilities across the whole grid. The second row has a normalization along the x-axis, while the third row has normalization along the y-axis. The predicted K-index is on the x-axis, while the observed one is on the y-axis. The darker the colored square, the more frequent the combination of forecasted and observed K-index occurs. Data from June 2004 on are included.

2.3.4 Error analysis

In this section a forecast is only treated as 'correct' if it exactly matches the observational value. Even if the forecast is higher than the observation, it is treated as erroneous (which is different from the treatment in part 3.5). Figure 11 indeed reflects large rmse values (and hence large errors) in the periods suggested by Figure 9 (2004, mid 2007 and begin 2011).

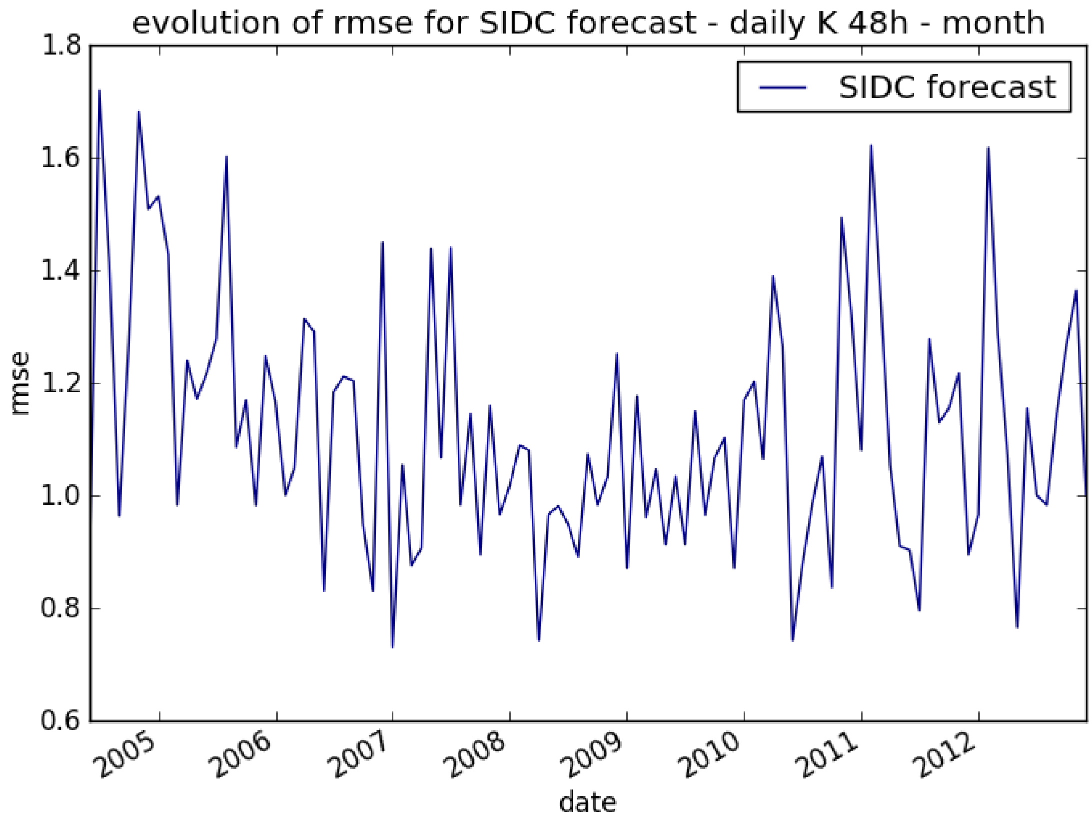

Fig. 11: Evolution of monthly rmse for the SIDC forecast.

2.3.5 Forecast verification of geomagnetic storms (K≥5) as binary event

The K-index is a parameter indicating the occurrence of a geomagnetic storm. It is essential to well predict such geomagnetic storm, independent of the severity. In this section we regard a geomagnetic storm as a binary event; it occurs or does not occur. A geomagnetic storm is defined for K≥5. For the analysis of binary events, several verification measures are introduced [Jolliffe and Stephenson]:

- A contingency table crosses the binary observational and forecast values (table 3). Using a contingency table, an observation can defined as a hit, miss, false alarm or correct rejection (see next bullet points).

		Observation	
		Yes (K≥5)	No (K<5)
Forecast	Yes (K≥5)	a	b
	No (K<5)	c	d

Table 3: Contingency table for a binary event.

- An event occurs when the observational K-index is equal to or larger than 5 (Observation=Yes). The number of events corresponds to $a + c$.
- The base rate of a sample is the proportion of events occurring; defined as $(a + c)/n$.
- A hit is a correctly forecasted event, which means both the observational and forecasted K-index are equal to or larger than 5. The number of hits is a.
- A miss is defined as an event that was not forecasted. The forecasted K-index is smaller than 5, while a K-index of at least 5 is observed. The number of misses corresponds to c.
- A false alarm is a forecast of an event (K≥5), while no event was observed (K<5). The number of false alarms is b.
- Correct rejection is a forecast of a non-event, while indeed no event was observed. The number of correct rejections is counted as d.
- Probability of Detection (POD) or hit rate is the ratio of the number of hits, divided by the number of events; calculated as $\frac{a}{(a+c)}$.
- Proportion Correctness (PC) is the ratio of total number of correct forecasts divided by the total number of forecasts; $\frac{(a+d)}{(a+b+c+d)}$.
- False Alarm Ratio (FAR) is a verification measure equal to the ratio of the number of false alarms by the total number of event forecasts; $\frac{b}{(a+b)}$.
- The Success Ratio (SR) is the complement of the false alarm ratio (FAR). It is calculated as the number of hits divided by the total number of event forecasts; $\frac{a}{(a+b)}$.
- Heidke Skill Score (HSS) is a skill score taking into account the number of correct random forecasts. HSS= (PC-E)/(1-E), with E=proportion of correct random forecasts, assuming forecasts and observations are independent and assuming the same proportion of forecasts of occurrence to non-occurrence. HSS has a range from -1 to 1, with 1 a perfect forecast, 0 as good as random and -1 the worst forecast.
- The True Skill Statistic (TSS) is a verification measure of categorical forecast similar to HSS. The TSS has nice characteristics for rare event forecasts. For example random and constant forecasts get a TSS of 0. For extremely rare events, TSS tends to converge to POD. TSS is calculated as $\frac{(ad-bc)}{((a+c)(b+d))}$. The TSS is also called the Peirce's skill score or the Hanssen and Kuipers' score.
- Bias is the degree of correspondence between the mean forecast and the mean observation; as such it indicates whether observations are over- or underestimated. For categorical forecasts, bias is defined as the ratio of the number of forecasts of occurrence to the number of actual occurrences: $B = \frac{(a+b)}{(a+c)}$.
- Critical Success Index (CSI) is a sample estimate of the conditional probability of a hit, given

that the event of interest was either forecast, observed or both. It is unsuitable as a performance measure for very common events, since the calculation is irrespective of the number of correct rejections. The CSI is an unreliable score, cause constant and random forecasts may result in different CSI values, depending on the proportion of forecast of occurrence to non-occurrence in the sample. A low CSI value can be improved artificially by forecasting occurrence at all times [Jolliffe and Stephenson]. The CSI is calculated as $\frac{a}{(a+b+c)}$.

- The Gilbert Skill Score (GSS) is an alternative to CSI that allows for the number of hits obtained purely by chance. The hits due to chance expected for forecasts independent of observations is given by: $ch = (a+b) * (a+c)/n$ and $GSS = \frac{(a-ch)}{(a+b+c-ch)}$. The skill scores GSS and HSS uniquely related as: $GSS = HSS/(2 - HSS)$ [Schaefer].

The most common verification measures are reported for each model forecasting the occurrence of geomagnetic storm (K≥5), both across all years as well as for each separate year. Table 4 shows these measures across all years and Figure 12 visualizes the evolution from 2004 to 2012 of some key verification measures for the same models.

	SIDC forecast	climatology	recurrence 14 days	recurrence 27 days	corrected recurrence 14 days	corrected recurrence 27 days
N	2950	2950	2950	2950	2950	2950
a	106	12	53	69	189	178
b	144	21	269	254	301	290
c	214	308	267	251	131	142
d	2486	2609	2361	2376	2329	2340
proportion hits	0.04	0.00	0.02	0.02	0.06	0.06
proportion false alarms	0.05	0.01	0.09	0.09	0.10	0.10
proportion misses	0.07	0.10	0.09	0.09	0.04	0.05
proportion correct rejections	0.84	0.88	0.80	0.81	0.79	0.79
base-rate s	0.11	0.11	0.11	0.11	0.11	0.11
POD	0.33	0.04	0.17	0.22	0.59	0.56
FAR	0.58	0.64	0.84	0.79	0.61	0.62
PC	0.88	0.89	0.82	0.83	0.85	0.85
SR	0.42	0.36	0.16	0.21	0.39	0.38
CSI	0.23	0.04	0.09	0.12	0.30	0.29
bias	0.78	0.10	1.01	1.01	1.53	1.46
GSS	0.18	0.02	0.03	0.06	0.24	0.23
HSS	0.31	0.05	0.06	0.12	0.39	0.37
TSS	0.28	0.03	0.06	0.12	0.48	0.45

Table 4: Performance measures for the different forecast models.

Figure 12 contains the POD and PC as intuitive measures. These scores clearly depend on the base rate. In case of very few events, e.g. in 2009 around solar minimum, the SIDC forecast has a very low POD, since it is very hard to predict these rare events. The PC was very high, since most non-events were predicted correctly. Hence, only using the PC could provide a false impression.

The lower panel of Figure 12 indicates that many events were missed in 2005, while proportionally this happened less in 2004 which is reflected in the PC. Also in other years as 2011 and 2012 many misses occur, but less false alarms were made, which returns a moderate PC.

TSS and HSS have very favorable statistical characteristics for the verification of forecast models [Jolliffe and Stephenson]. A main difference between TSS and HSS is that TSS has the property being independent on the base-rate, while HSS treats 'misses' and 'false alarms' equally.

The corrected recurrence models have a better HSS and TSS value than the SIDC forecast, indicating these models can better estimate a geomagnetic storm. This is in correspondence to Figure 10, showing only few underestimations of the K-index by the corrected recurrence models. The SIDC forecast still has higher HSS and TSS scores than the climatology and (uncorrected) recurrence models.

At a base rate s<1/2 (which is the case here), the TSS treats overestimating models (i.e. with a high bias) more generously than HSS and underestimating models more harshly. This is reflected in the fact that the overestimating corrected recurrence models obtain a high TSS value, while the HSS values are closer to each other (see Table 4).

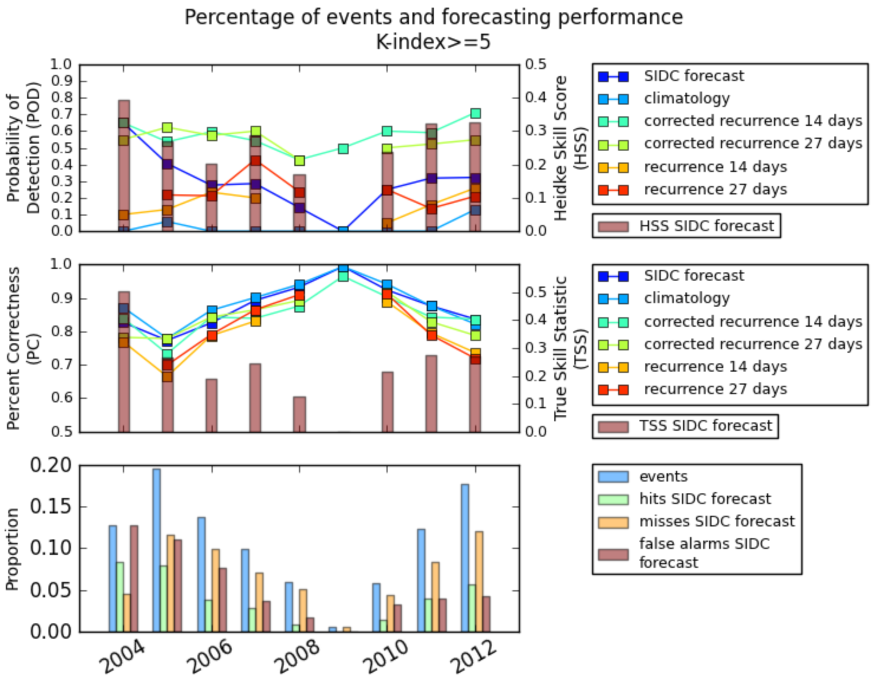

Fig. 12: Verification measures of the SIDC forecast and models to predict a geomagnetic storm with K at least 5, across the years from 2004 on. Measures are the probability of detection (POD, top panel) and proportion correctness (PC, middle panel) for all forecasts, and the Heidke Skill Score (HSS, top panel) and the True Skill Statistic (TSS, middle panel) for the SIDC forecast.
The lower panel visualizes the proportion of days with an event, a hit, a miss and a false alarm. The proportion of hits and the proportion of misses sum up to the number of events.

2.4 Conclusions and next steps

The reported analysis aids to identify the strong and weak points of RWC forecasting as well as those of the models considered. The analysis will be rerun every year. As such, it creates the opportunity to continuously reevaluate and increase the reliability of space weather forecasting.

At SIDC, the F10.7 flux is very well forecasted on day 1 compared to other models, but rather poor on days 2 and 3. The manual forecasting at SIDC generally overestimates the flux, while the corrected recurrence models on average provides underestimations. The largest errors occur at observed flux values above 200, corresponding to very high solar activity.

The estimation of local geomagnetic index K provided for the next 48 hours results in a distribution similar to that of the observations. Only the extreme values $K = 0$ and $K \geq 7$ are hardly forecasted, resulting in an underestimation of the strong events. The corrected recurrence models provide a much flatter distribution, by estimating the extreme K-values too often.

By converting the geomagnetic K-index in a binary format, the forecasting of a geomagnetic storm ($K \geq 5$) is evaluated. In several years since the K-index is forecasted at SIDC, a large proportion of false alarms and misses occurs. However, compared to the corrected recurrence models the proportion of false alarms is lower and the proportion of misses is only slightly higher.

The described verification analysis is currently being extended to the forecasts of solar flare probabilities. Also other ideas such as the influence of the forecaster and more in-depth error analysis for the K-index are under investigation.

2.5 General comments

All code is written in Python 2.7 and using packages matplotlib1.1.0, scipy 0.10.1, numpy 1.6.1 and pandas 0.8.0. The program will be run yearly to update the output on the SIDC website (http://www.sidc.be/forecastverification).

3. Validation activities at SWPC

This section describes the AFFECTS related validation activities at the Space Weather Prediction Center (SWPC) of the National Oceanic and Atmospheric Administration (NOAA). This covers the SWPC contributions to the AFFECTS project for the second year activities. There are several areas where validation is underway or planned. These are listed here

1. Validation of the Early Warning Message
2. Solar Flare and Solar EUV irradiance.
3. CME Parameterization: Identification of key parameters of the CME which determine the forecast arrival time (and strength?) at ACE.
4. Solar EUV Irradiance: Comparing various solar EUV irradiance measurements and proxies to better specify and forecast the solar irradiance relevant to ionospheric products and services.
5. Validation of ionospheric parameters such as TEC: Comparing SWACI with USTEC and CTIPe to better understand and validate model performance

6. Validation of the location of the auroral boundary: Comparing aurora specification and forecast models with ground magnetometer chain to quantify the location of the aurora and validate specification and forecasts of the aurora.

3.1 Validation of the Early Warning Message

The Early Warning Message provides general information on impending space weather that may impact radio communication and navigation. The message includes

a. Onset time and peak flux of major (M- and X- Class) X-ray flares and equivalent EUV flares.
b. Flux of solar energetic protons
c. Onset time, source region location, speed, direction, width, arrival time, and shock strength
d. Geomagnetic storm magnitude
e. Reliability or error of warning

The Early Warning Message is both a specification and a forecast of space weather. The parameters provided in the Message will be compared to observations to validate the forecasts and confirm their accuracy and reliability.

3.2 X-Ray and EUV Flare Observations

The Early Warning Message provides detailed information on the onset time and peak flux of major flares. The Onset Time, Peak Flux, Peak Flux Time, and Flare Duration are standard products from the NOAA Space Weather Prediction Center. Events are collected into daily files and placed on the SWPC FTP web site at http://www.swpc.noaa.gov/ftpdir/indices/events/. The Table 5 below shows the X-ray information for seven flares on 12 December, 2012. The columns are "Event Number", "Begin Time", "Time of Maximum", "End Time", "Observation Satellite" (GOES 15), "Observation Type" (X-Ray), "Flare Magnitude", and "Integrated Flux" (J-m/E^2). This information is readily available and will be used to validate the AFFECTS Early Warning Message.

Event #	Begin	Max	End	Obs.	Type	Channel	Mag.	Int. Flux
7860	0111	0115	0120	G15	XRA	1-8A	B5.5	2.10E-04
7910	1044	1047	1049	G15	XRA	1-8A	B6.4	9.50E-05
7950	1452	1455	1458	G15	XRA	1-8A	B5.4	1.20E-04
7960	1518	1521	1523	G15	XRA	1-8A	B5.3	8.70E-05
7990	2028	2103	2132	G15	XRA	1-8A	C1.1	3.60E-03
8000	2207	2211	2215	G15	XRA	1-8A	C1.0	3.30E-04
8010	2320	2323	2325	G15	XRA	1-8A	B6.5	1.10E-04

Table 5: Sample of X-ray Flares from the "Edited Events" file for 12 Dec. 2012. Times are given in UT.

In addition to the x-ray flux, the Early Warning Message will contain information on the timing and magnitude of the Extreme Ultraviolet (EUV) flare. This can be validated against a number of solar EUV observations including the GOES EUVS, the SOHO SEM, and the SDO EVE sensors. Figure 13 shows comparisons of the daily values of solar EUV irradiance at the He 30.4 nm wavelength.

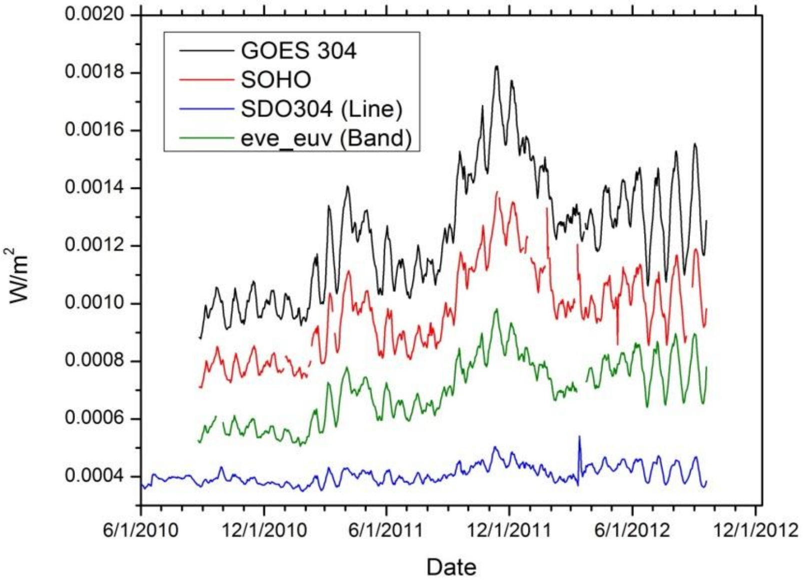

Fig. 13: Validation of solar EUV irradiance values from several sensors on three different satellites.

Forecasting solar EUV: The solar EUV irradiance is one of the critical inputs that drive ionospheric variability. Much of the effort in the AFFECTS project is focused on forecasting the other main energy input to the ionosphere, the solar wind-driven geomagnetic storm. The NOAA Space Weather Prediction Center provides three day forecasts of the F10.7 cm flux which is a commonly used proxy for solar EUV. But it may be possible to get better forecasts using the actual EUV irradiance. A simple model has been developed which relies primarily on "persistence" for forecasting the solar irradiance. The concept is that the solar flux of today, is very similar to that of 27 days ago (one solar rotation). Also, the variability of the flux over the next few days will be similar to that of the previous rotation. Using this concept, it is straight forward enough to forecast the solar EUV irradiance for the next few days. Figure 14 shows a plot of the daily averaged solar EUV irradiance at three wavelengths. A five-day forecast is calculated by scaling the current daily value to the daily value from 27 days ago and then propagating forward in time.

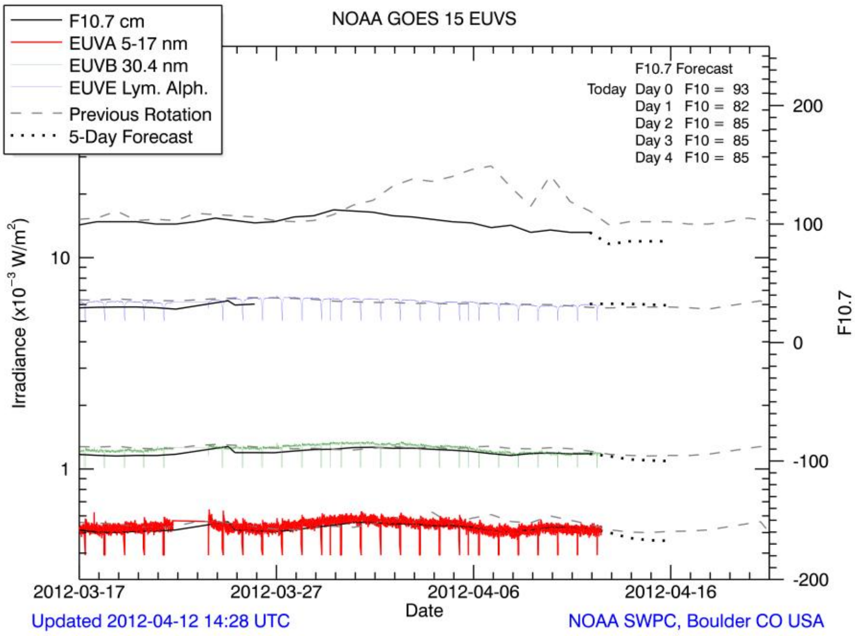

Fig. 14: Solar EUV irradiance observations and forecasts.

3.3 Proton Flux Forecasts

The forecast of energetic proton events is one of the most challenging aspects of space weather prediction. Energetic protons penetrate into Earth's upper atmosphere, especially near the poles, ionizing the upper atmosphere and creating anomalous layers in the lower ionosphere. The enhanced ionosphere absorbs HF radio waves blocking radio communication. Forecasts of the solar energetic proton events will be validated against the observed proton flux at the NOAA GOES spacecraft in geosynchronous orbit. GOES proton observations are used to define the magnitude, timing, and duration as well as the spectral characteristics of a proton event.

3.4 CME Characterization

Coronal Mass Ejections carry the bulk of the energy that creates geomagnetic storms which block HF radio transmissions and disrupt GPS/GNSS navigation systems. Characterization of the CME near the sun can provide a 1-3 day lead time in forecasts of geomagnetic storms. Several characteristics of a CME will determine whether it will impact Earth and how large the impact will be. The source location on the sun, the direction of travel and the angular size of the CME are determined to predict if the CME will strike Earth. The speed of the CME will provide information on the arrival time and timing of the resulting geomagnetic storm. The density of the CME and the internal magnetic field structure (direction and strength) will determine how geo-effective the CME will be when it arrives at Earth. Each of these parameters will be measured near the sun and a forecast of the timing and magnitude of the event will be generated. The forecast will be validated by monitoring the solar wind conditions near Earth (from the ACE and DSCOVR satellites) to determine the timing and internal structure of the CME.

3.5 Geomagnetic Storm Magnitude and Impacts

Ultimately, the goal of the AFFECTS project is to provide customers with information on the near-Earth geomagnetic and ionospheric conditions. The key will be to validate the forecast of the geomagnetic storm and the impacts on ionosphere and communication and navigation.

The aurora is an indicator of where the ionosphere will be most disturbed and thus the location of the potential for blocked radio communication and disrupted GNSS navigation. The University of Tromso magnetometer chain will provide observations not only of the strength of the storm but also of the location of the auroral boundary as the auroral oval expands away from the poles. Customers of course request forecasts of these conditions. We introduce the Auroral Boundary Model (ABM) as a new product. This model was developed by [Carbary] to specify the polward and equatroward boundaries of the aurora and the latitude and magnitude of peak intensity. It is driven by the Kp geomagnetic index. Thus the three-day forecasts of Kp, provided at a 3-hour cadence, will allow us to provide forecasts of the aurora with up to three days of lead time. We will use the Auroral Electrojet Tracker to validate the ABM model performance. Figure 15 shows the Auroral Electrojet Tracker with the aurora from the ABM model overlaid upon it. This activity is still under development so this figure is more of a notional representation of what we might be able to produce.

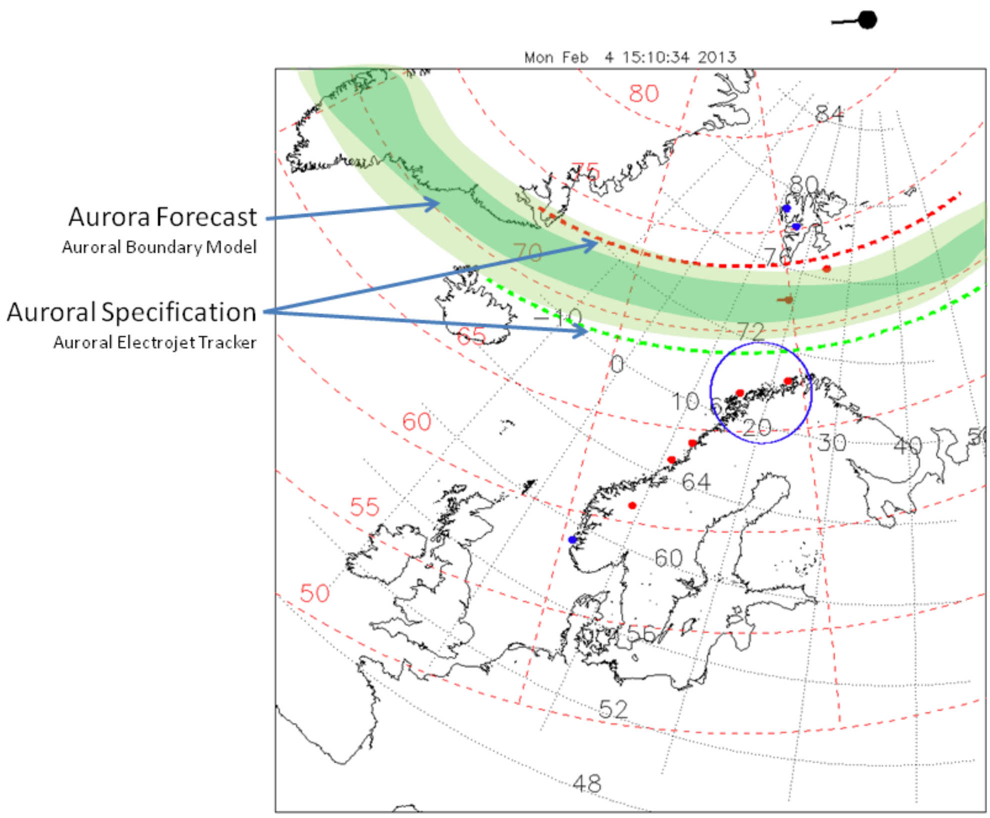

Fig. 15: By comparing the location of the aurora provided by the Auroral Boundary Model, with the observed location of the aurora provided by the Auroral Electrojet Tracker model, we can validate the aurora forecasts.

For the GPS/GNSS community, the height integrated Total Electron Content (TEC) is an excellent proxy for ionospheric disturbances that modify the GPS/GNSS signal and increase the positioning error for the user. Global maps of TEC produced by the DLR-SWACI model will be one of the most important products from the AFFECTS project. Validation of these maps will be critical in establishing the validity and quantifying the accuracy of the forecasts. To validate the DLR-SWACI global TEC maps and to develop estimates of errors and uncertainties, it is necessary to compare them with other global maps of TEC as well as local observations. A web site has been developed (http://helios.swpc.noaa.gov/ctipe) where several models, both assimilative and physics-based, are displayed in real-time for validation and comparison. Under the validation tab at this web site, there are comparisons between several models. The NOAA Coupled Thermosphere Ionosphere Plasmasphere with electrodynamics (CTIPe) model is a physics based model of the thermosphere/ionosphere. The NOAA US Total Electron Content (USTEC) model is an assimilative model with extensive data inputs. Under the DLR tab are the results of the DLR-SWACI model which is an assimilative model of global TEC. There is also the US Air Force Global Assimilative Ionospheric Model (GAIM) which is the operational model used by the US Air Force for forecasting the ionosphere. Each of these models uses different data and different assimilation techniques to derive the same quantities.

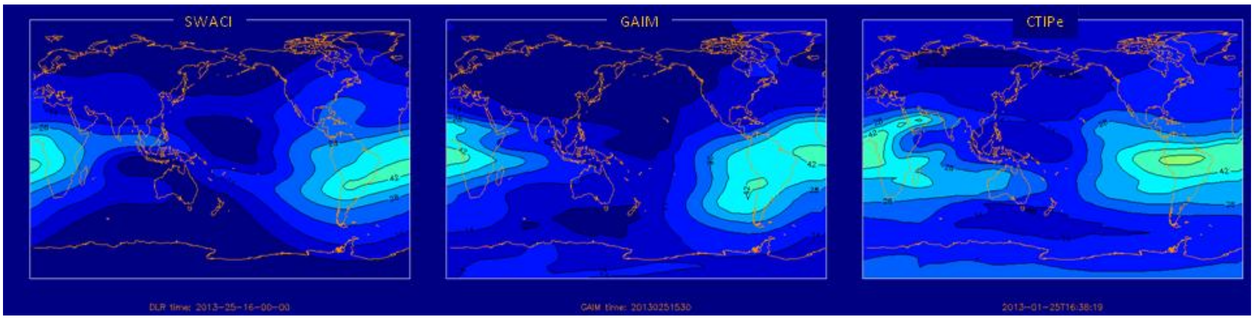

Fig. 16: Comparing global models of TEC. The three models DLR-SWACI, US Air Force GAIM, and NOAA CTIPe are shown from left to lower right.

To further assess model performances, differences between models are calculated to quantify the variations. In Figure 16, the DLR-SWACI is compared with the assimilative USTEC model over the United States. Both models use the International Reference Ionosphere (IRI) as the background global model into which ground GPS data are assimilated. The USTEC model is considered to be quite accurate over the US because of the density of data that is used to drive the model. There are significant differences between the models and further analysis is required to determine the source of these differences and identify the true errors and uncertainties.

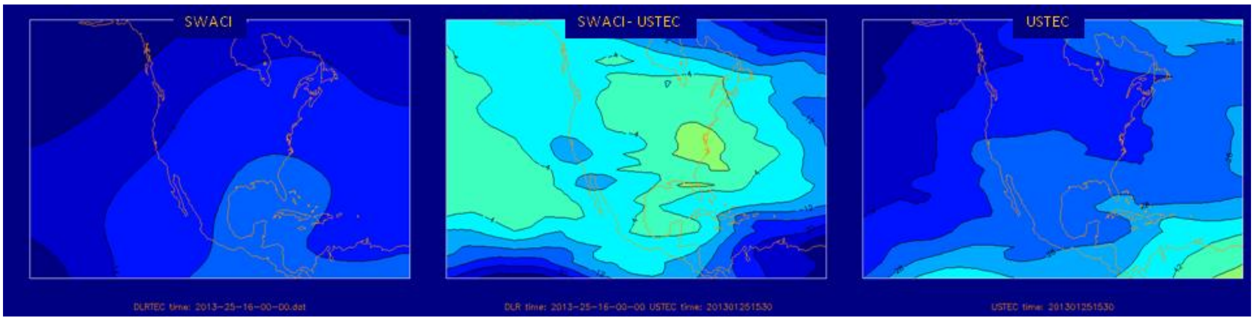

Fig. 17: Comparing the DLR-SWACI model (left) with the USTEC model (right) by taking the difference between the two models (center) over the US.

4. User Feedback at the AFFECTS User Workshop

4.1 Sample of respondents

At the AFFECTS User Workshop on February 28, 2013 a questionnaire was distributed to the attendees. Fifteen attendees have provided their answers. The responses concerning the AFFECTS products are described below.

Eight of the respondents were involved in the AFFECTS project, four others were staff from ROB or STCE, one from BISA, one from ESA/ESOC and one respondent was an aurora hunter organizing aurora tourism.

4.2 Interest in space weather products

Eleven out of fifteen use the alerts and forecasts of SIDC, out of which five are also interested in bulletins. Two others are using either the NOAA products or require data for own analysis. One single person expresses no specific interest in space weather products but rather all customer requirements.

Majority of the sample (twelve out of fifteen) is interested in products with solar, CME and geomagnetic information. Seven want aurora information and four are asking for ionospheric products. One person uses only geomagnetic, aurora and solar wind data.

Related to the time scale, most respondents require forecasts for the next 24 hours, but for three persons a time scale of a few hours is also very useful. The respondents involved in forecasting like to look on a range of three days or longer.

AFFECTS products and services	Amount of interested respondents (on 15)	Frequency
ROB-SIDC SW forecasts	13	Daily (1 resp: also hourly)
NOAA-SWPC SW forecasts	12	Daily (1 resp: also hourly)
Alerts on the AFFECTS website	5	Daily (1 resp: also hourly)
Solar Demon dimming and EIT wave detector	7	Daily (1 resp: also hourly, 1 resp: weekly)
STAFF viewer	10	Daily
L1 solar wind, Kp, auroral and GPS error alert	6	Daily
Real-time CME, Kp, Aurora, GPS error forecast	5	Daily
Geomagnetic forecast tool by SRI-NASA-NSAU	8	Daily (1 pers: weekly, 1 resp: also hourly)
Early Warning for GNSS Users	1	
Other...	Presto (cfr ROB-SIDC SW forecasts) GCS mesh for CME, auroral oval over Europe: via AFFECTS website	Daily (1 resp: also hourly)

Table 6: Overview of the interest in space weather products

As illustrated in Table 6, the forecast and alert products are most popular, while the messages for geomagnetic activity are of lesser interest. This is largely caused by the sample of the respondents; mainly consisting of researchers developing space weather products themselves. Only one 'real' end user responded, interested in aurora. Note that the Early Warning for GNSS Users is still in the commissioning phase and hence has no users yet.

Most products are required on a daily basis. Two persons like to receive the AFFECTS products on a time scale which is feasible according to the state of the art. The aurora hunter uses the products daily but only in the winter season of Lapland.

Only four persons would require a user manual, two of them asking for expert assistance for the installation of specific products. Two users let their interest in a user manual depend on the product. A single respondent asks for illustrated examples for interpretation of specific products.

4.3 Suggestions for improvements or new products

Several respondents provide suggestions for improvements to the AFFECTS products, such as:

- Improve stability of STAFF (now it might crash)
- Add simple statistics/calculator to STAFF.
- Automatic Bz-scaling in STAFF
- Separate graphs for observations from Sun - Solar Wind - Earth
- Add alerts on CH, HCS, CIR alerts to Presto
- Indication of errors on forecast
- Simplified output for non-expert users on what might be the effect on Earth

Some ideas for new products were also given:

- In case of only one viewing direction, a cone-like shape should be used to derive the propagation direction of a CME
- Hourly forecast of solar wind at L1 based on STEREO observations and WSA-Enlil simulations

The following suggestions were made outside the scope of AFFECTS:

- Forecast of the direction and strength of IMF, density of the solar wind and velocity at Earth's orbit
- Development of portable magnetometers

4.4 Main outcome of the survey

Almost all respondents of this survey are directly involved in the space weather community, mostly as researchers or developers of space weather products. The sample is atypical because of the limited number of end users such as satellite and flight operators, power grid exploitants, GPS/GNSS users, which introduces a bias.

The respondents mentioned the products and timing of highest interest and provided suggestions for improvements to the AFFECTS products. Some improvements can be elaborated within the framework of the project, while others should be elaborated on a longer term.

5. References

Carbary, J.F., A Kp-based model of auroral boundaries, Space Weather, 3, 10, CiteID S10001, 2005.

Chatterjee, S. and A.S. Hadi, Influential Observations, High Leverage Points, and Outliers in Linear Regression, Statistical Science, 1, No. 3, 379-416, 1986.

Jolliffe, I.T. and D.B. Stephenson, Forecast Verification. A practitioner's Guide in Atmospheric Science, 2nd edition, Wiley-Blackwell, 2012.

Schaefer, J.T., The Critical success index as an indicator of warning skill, Weather Forecast, 5, 570-575, 1990.

SIDC-team, World Data Center for the Sunspot Index, Royal Observatory of Belgium, Monthly Report on the International Sunspot Number, online catalogue of the sunspot index: http://www.sidc.be/sunspot-data/.

Tapping, K.F., and D.P. Charrois, Limits to the accuracy of the 10.7 cm flux, Solar Physics, 150,305-315, 1994.

6. Appendix

6.1 List of Acronyms

ABM	**A**uroral **B**oundary **M**odel
ACE	**A**dvanced **C**omposition **E**xplorer
AFFECTS	**A**DVANCED **F**ORECAST **F**OR **E**NSURING **C**OMMUNICATIONS **T**HROUGH **S**PACE
AR	**A**ctive **R**egion
BISA	**B**elgian **I**nstitute for **S**pace **A**eronomy
CH	**C**oronal **H**ole
CIR	**C**orotating **I**nteraction **R**egion
CR	**C**arrington **R**otation
CME	**C**oronal **M**ass **E**jection
CSI	**C**ritical **S**uccess **I**ndex
CTIPe	**C**oupled **T**hermosphere **I**onosphere **P**lasmasphere with **e**lectrodynamics
DLR	**D**eutschen Zentrums für **L**uft- und **R**aumfahrt (in English: German Aerospace Center)
DSCOVR	**D**eep **S**pace **C**limate **O**bser**v**ato**r**y
ESA	**E**uropean **S**pace **A**gency
ESOC	**E**uropean **S**pace **O**perations **C**entre
EUV	**E**xtreme **U**ltra**v**iolet
EUVS	Solar **E**xtreme **U**ltra**v**iolet **S**ensor on GOES
EVE	**E**xtreme Ultraviolet **V**ariability **E**xperiment on SDO
FAR	**F**alse **A**larm **R**ate
GAIM	**G**lobal **A**ssimilative **I**onospheric **M**odel
GCS	**G**raduated **C**ylindrical **S**hell

GOES	Geostationary Satellite system
GNSS	**G**lobal **N**avigation **S**atellite **S**ystems
GPS	**G**lobal **P**ositioning **S**ystem
GSS	**G**ilbert **S**kill **S**core
HF	**H**igh **f**requency
HCS	**H**eliospheric **C**urrent **S**heet
HSS	**H**eidke **S**kill **S**core
IMF	**I**nterplanetary **M**agnetic **F**ield
ISN	**I**nternational **S**unspot **N**umber
IQR	**i**nter**q**uartile **r**ange
IRI	**I**nternational **R**eference **I**onosphere
mse	**m**ean **s**quared **e**rror
NOAA	**N**ational **O**ceanic and **A**tmospheric **A**dministration
nT	**n**ano**t**esla
PC	**P**roportion **C**orrectness
POD	**P**robability **o**f **D**etection
rmse	**r**oot **m**ean **s**quared **e**rror
ROB	**R**oyal **O**bservatory of **B**elgium
RWC	**R**egional **W**arning **C**enter
SDO	**S**olar **D**ynamics **O**bservatory
SEM	**S**olar **E**xtreme Ultraviolet **M**onitor on SOHO
sfu	**s**olar **f**lux **u**nit
SOHO	**So**lar and **H**eliospheric **O**bservatory
SIDC	**S**olar **I**nfluences **D**ata analysis **C**enter
Solar **Demon**	Solar **D**imming and **E**UV wave **Mon**itor
SR	**S**uccess **R**atio
SRI-NASA-NSAU	**S**pace **R**esearch **I**nstitute of **NASU-NSAU**
SSN	**S**moothed **S**unspot **N**umber
STAFF	**S**olar **T**imelines viewer for **AFF**ECTS
SW	**S**pace **W**eather
SWACI	**S**pace **W**eather **A**pplication **C**enter - **I**onosphere
SWPC	**S**pace **W**eather **P**rediction **C**enter
TEC	**T**otal **e**lectron **c**ontent
TSS	**T**rue **S**kill **S**tatistic
USTEC	**US** **T**otal **E**lectron **C**ontent
WSA	**W**ang-**S**heeley-**A**rge